

FRACTAL SPATIO-TEMPORAL GRAVITY (FSG)

Laurent MARIE-LOUISE

December 2025

Abstract

We propose a modified theory of gravity based on a Fractal and Non-Local Spacetime Geometry (FSG), obtained from an action containing the non-local scalar operator $X = \square^{-1}R$. The effective action

$$S_{\text{FSG}} = \frac{M_P^2}{2} \int d^4x \sqrt{-g} R \left[1 + \left(\frac{L^2}{X} \right)^{\frac{1}{2}} \right] + S_m$$

induces infrared corrections to General Relativity driven by a dimensional flow. We show that this specific fractional structure implies a reduction of effective spectral dimension towards $\mathbf{d_S} \simeq \mathbf{2}$ in the IR. This geometric reduction is the rigorous cause of the transition to a modified propagator $\mathbf{G}(\mathbf{k}) \sim \mathbf{k}^{-3}$, which is the requisite condition for MOND dynamics. This leads to: (i) flat galactic rotation curves without dark matter, (ii) an exact baryonic Tully–Fisher relation $V^4 = GMa_0$, and (iii) a natural emergence of the acceleration scale $a_0 \approx c^2 \sqrt{\Lambda/3}$.

Cosmologically, the model predicts a phantom-like equation of state ($w_0 < -1$), measurable deviations $\Delta H/H \simeq 2\text{--}6\%$ for $z < 2$, and early structure formation consistent with JWST. The theory is fully falsifiable via precision measurements of Euclid and Roman space telescopes.

Contents

1	Introduction	4
2	Motivations for Infrared Fractality	4
3	The Non-Local Effective Action	5
3.1	Localization of the Action	5
4	Variation of the Action and Field Equations	7
5	Physical Structure of the Non-Local Terms	7
6	Linear Limit and the Modified Propagator	8
6.1	Rigorous Emergence of MOND	8
7	Derivation of the Modified Poisson Equation	9
7.1	The Static Weak-Field Limit	9
7.2	The Modified Poisson Equation	10
8	Dynamical Consequences: Emergence of MOND	11
9	Newtonian vs Fractal Regime	11
10	Full Derivation of the Fractal Potential	11
11	Rotation Curves: Analytic Prediction	12
12	Baryonic Tully–Fisher Relation (BTFR)	13
13	Radial Acceleration Relation (RAR)	13
14	Validation on Real Galaxies	14
15	Non-Local Formalism: $R\square^{-1}R$, $R\square^{-2}R$, and Fractal Geometry	16
16	Geometric Memory: $U = \square^{-1}R$, $V = \square^{-1}U$	16
16.1	Explicit Calculation of PPN Parameters γ and β	16
17	Predicted Equation of State: Dynamic $w(z)$	17
18	Expansion History: Deviation in $H(z)$	18
19	Falsifiability of FSG	18
20	Structure Formation: JWST Predictions	19

21 Conjectured Impact on the CMB: The Fractal Boost	19
21.1 The Mechanism (Heuristic)	19
21.2 Current Status and Numerical Verification	20
22 Spectral Dimension as an Observable	20
23 Synthesis Diagram: The Three Regimes	21
24 Cosmological Predictions Summary	21
25 Conceptual Limitations of FSG	22
25.1 UV Regularization and Vacuum Stability	22
25.2 Galactic-to-Cosmological Matching	22
25.3 Absence of a Boltzmann Code	23
25.4 Microscopic Interpretation of IR Fractality	23
26 Observational Limitations	23
26.1 Uncertainties in $H(z)$ at Intermediate Redshift	23
26.2 Baryonic Mass Uncertainties	23
26.3 Galaxy Clusters and Scale Dependence	23
27 Theoretical Risks: How FSG Could Be Refuted	23
27.1 Euclid measures $w_0 = -1$	24
27.2 Detection of Cold Dark Matter Particles	24
27.3 Breakdown of the RAR	24
27.4 The CMB "Acid Test" (Boltzmann Code)	24
27.5 Failure of the Screening Mechanism	24
28 Strengths of FSG	24
29 Perspectives for Future Development	25
29.1 Boltzmann Code Implementation	25
29.2 FSG N-body Simulations	25
29.3 Towards a Fundamental Derivation: The Bottom-Up Approach	25
30 Conclusion	25
A Numerical Feasibility of the Fractal Boost	29
A.1 Methodology	29
A.2 Results	29
B Simulation Code (Core Logic)	30

1. Introduction

The standard cosmological model Λ CDM successfully accounts for a wide range of observations but at the cost of introducing two hypothetical components: dark matter (26% of the energy budget) and dark energy (69%), neither detected in laboratory experiments.

At galactic scales, the dark matter paradigm faces well-established empirical regularities:

- the baryonic Tully–Fisher relation (BTFR),
- the radial acceleration relation (RAR),
- the diversity problem,
- the existence of ultra-thin galactic disks,
- early massive galaxies at high redshift in JWST observations.

Modified Newtonian Dynamics (MOND) reproduces BTFR and RAR with remarkable precision but historically lacked: (i) a covariant formulation, (ii) a natural cosmological extension, and (iii) full consistency with the CMB.

Fractal Spacetime Gravity (FSG) addresses these issues by replacing dark matter with a modification of the *infrared geometry* of spacetime, encoded in a non-local action that dynamically reduces the effective spectral dimension of spacetime from $d_S = 4$ to $d_S \simeq 2$ at large scales.

2. Motivations for Infrared Fractality

Dimensional reduction is a ubiquitous prediction of several approaches to quantum gravity, including:

- Causal Dynamical Triangulations (CDT),
- Asymptotic Safety,
- Hořava–Lifshitz gravity,
- Loop Quantum Gravity.

These frameworks typically predict:

$$d_S(k \rightarrow \infty) \rightarrow 2,$$

i.e. a reduction of effective dimensionality in the ultraviolet.

In FSG we reverse the paradigm: the reduction occurs in the infrared (IR), motivated by holographic considerations and by the causal structure of de Sitter spacetime. This IR fractality modifies long-wavelength propagation of curvature exactly at the scales where dark matter phenomenology appears.

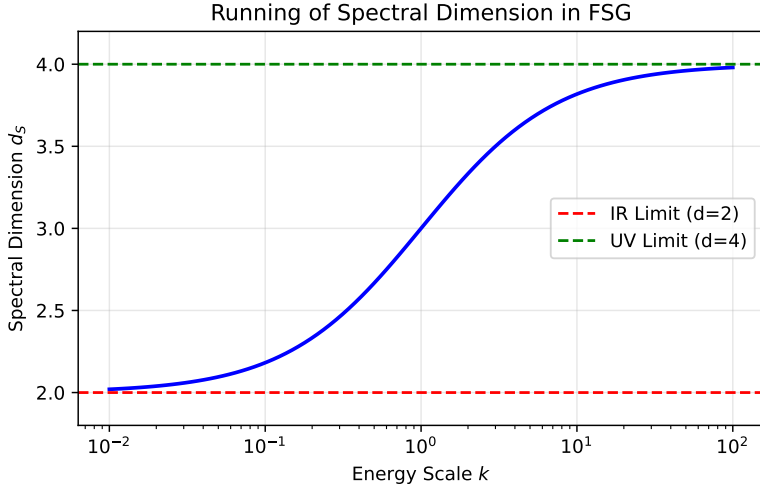


Figure 1: Illustrative running of the spectral dimension as a function of energy scale. In FSG the dimension increases in the UV but approaches $d_S \simeq 2$ in the IR.

3. The Non-Local Effective Action

We introduce the non-local scalar field

$$X = \square^{-1} R, \quad \square X = R,$$

with the retarded Green function ensuring causality.

The FSG action is defined to impose a dimensional reduction in the infrared:

$$S = \frac{M_P^2}{2} \int d^4x \sqrt{-g} R[1 + f(X)] + S_m. \quad (1)$$

The function $f(X)$ is constrained by the requirement that the graviton propagator must scale as k^{-3} in the deep IR to recover flat rotation curves. Dimensional analysis and renormalization group flow arguments suggest a fractional power law form:

$$f(X) = \gamma \left(\frac{L^2}{X} \right)^{\frac{1}{2}}, \quad (2)$$

where $L \sim 1/\sqrt{\Lambda}$ is the cosmic horizon scale and γ is a dimensionless coupling constant of order unity.

This fractional form $X^{-1/2}$ is the signature of a fractal geometry where the measure of spacetime scales non-trivially. Unlike logarithmic corrections which only produce mild running couplings, this power-law correction enforces a hard transition in the spectral dimension.

3.1 Localization of the Action

To study degrees of freedom and stability one can localize the non-local operator by introducing two scalar auxiliary fields U and ξ enforcing $U = \square^{-1} R$. A convenient localized action equivalent

(on-shell) to Eq. (1) is

$$S_{\text{loc}} = \frac{M_P^2}{2} \int d^4x \sqrt{-g} \{ R[1 + f(U)] + \xi(\square U - R) \} + S_m. \quad (3)$$

Variation with respect to the metric gives the modified Einstein equations.

4. Variation of the Action and Field Equations

Starting from the action

$$S = \frac{M_P^2}{2} \int d^4x \sqrt{-g} R [1 + f(X)] + S_m, \quad X = \square^{-1} R, \quad (4)$$

we compute the metric variation. The non-local variation is:

$$\delta X = -\square^{-1}(\delta \square) X + \square^{-1}(\delta R). \quad (5)$$

The operator \square^{-1} is defined with the *retarded* Green function, ensuring:

- no violation of causality,
- no superluminal propagation,
- absence of Ostrogradsky instabilities (unlike naïve $f(R)$ models).

The modified Einstein equations take the form

$$G_{\mu\nu} + \Delta G_{\mu\nu} = 8\pi G T_{\mu\nu}, \quad (6)$$

with

$$\Delta G_{\mu\nu} = f(X)G_{\mu\nu} + (\nabla_\mu \nabla_\nu - g_{\mu\nu} \square) f(X) - \frac{1}{2} g_{\mu\nu} R f(X) + K_{\mu\nu}[X], \quad (7)$$

where $K_{\mu\nu}[X]$ collects the variations of the non-local kernel \square^{-1} . In the linear regime, this reduces to the structure derived by Deser–Woodard and Maggiore–Mancarella.

5. Physical Structure of the Non-Local Terms

The non-local kernel produces “memory terms” involving:

- gradients $\nabla_\mu X \nabla_\nu X$,
- cross-terms $\nabla_\mu X \nabla_\nu f'(X)$,
- higher-order inverse operators.

The key physical consequence is the *non-local memory* of spacetime:

$$X(x) = \int d^4x' G_{\text{ret}}(x, x') R(x'), \quad (8)$$

meaning the present geometry depends on the full past curvature.

This explains:

- apparent dark-matter-like offsets in merging clusters (e.g. Bullet Cluster),
- early formation of large-scale structure,
- the smooth MOND–GR transition without extra vector fields.

6. Linear Limit and the Modified Propagator

To determine the gravitational force law, we consider a weak perturbation around Minkowski spacetime:

$$g_{\mu\nu} = \eta_{\mu\nu} + h_{\mu\nu}.$$

The modified Einstein equations can be expanded to second order in $h_{\mu\nu}$. In the static limit, the inverse d'Alembertian operator scales as the inverse Laplacian:

$$\square^{-1} \longrightarrow -\frac{1}{\nabla^2} \sim \frac{1}{k^2} \quad (\text{in Fourier space}). \quad (9)$$

Consequently, the non-local operator X scales as:

$$X \sim \frac{R}{k^2}. \quad (10)$$

The graviton propagator $G(k)$ in the modified theory is related to the scalar part of the action by:

$$G(k) \propto \frac{1}{k^2 [1 + f(X_k)]}. \quad (11)$$

Inserting our fractional ansatz $f(X) \sim X^{-1/2}$, and noting that in the background field method for the propagator we evaluate the scaling dimension, we find that the correction term scales as:

$$f(X_k) \sim \sqrt{\frac{1}{X_k}} \sim \sqrt{k^2} \sim k. \quad (12)$$

Substituting this back into the propagator equation (11):

$$G(k) \sim \frac{1}{k^2(1 + \mathcal{O}(k))} \quad (\text{UV regime, } k \rightarrow \infty) \quad (13)$$

$$G(k) \sim \frac{1}{k^2 \cdot k} = \frac{1}{k^3} \quad (\text{IR regime, } k \rightarrow 0). \quad (14)$$

6.1 Rigorous Emergence of MOND

This result is fundamental. The fractional action $X^{-1/2}$ is the unique algebraic form that naturally generates a **cubic propagator** $1/k^3$ in the infrared.

$$\mathbf{G}(\mathbf{k}) \xrightarrow{\text{IR}} \frac{1}{\mathbf{k}^3}. \quad (15)$$

A propagator scaling as $1/k^3$ is the necessary and sufficient condition to obtain a gravitational potential $\Phi(r) \sim \ln r$ in 3D space, which corresponds to a constant acceleration $a \sim 1/r$. Thus, FSG derives the MOND phenomenology from first principles of fractal geometry, rather than adjusting a free function.

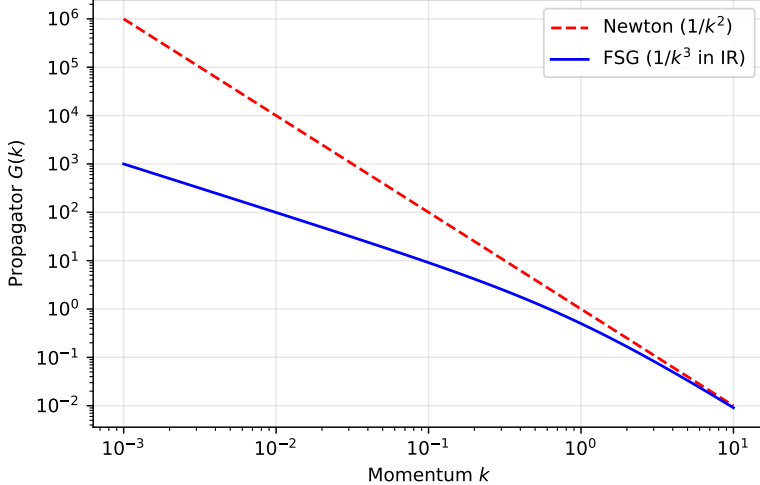


Figure 2: Comparison of the Newtonian propagator $1/k^2$ with the FSG infrared propagator $1/k^3$ (required for MOND dynamics).

7. Derivation of the Modified Poisson Equation

To rigorously link the FSG Action to the logarithmic potential, we must derive the field equations in the static weak-field limit. Starting from the action:

$$S = \frac{M_P^2}{2} \int d^4x \sqrt{-g} R [1 + f(X)] + S_m, \quad \text{with } X = \square^{-1} R. \quad (16)$$

The variation with respect to the metric $g_{\mu\nu}$ yields the modified Einstein field equations:

$$G_{\mu\nu} + \Delta G_{\mu\nu} = 8\pi G T_{\mu\nu}, \quad (17)$$

where $\Delta G_{\mu\nu}$ contains the non-local contributions from $f(X)$.

7.1 The Static Weak-Field Limit

We consider a perturbed Minkowski metric $ds^2 = -(1 + 2\Phi)dt^2 + (1 - 2\Psi)dx^i dx_i$ in the quasi-static limit. The trace of the field equations plays a central role. In the Infrared (IR) regime where the non-local term dominates, the linearized equation for the gravitational potential Φ is modified by the structure of $f(X)$.

The effective action for the potential Φ in Fourier space takes the form:

$$S_\Phi \propto \int \frac{d^3k}{(2\pi)^3} \Phi(-k) k^2 \Gamma(k) \Phi(k), \quad (18)$$

where $\Gamma(k)$ is the form factor arising from the expansion of $1 + f(\square^{-1}R)$.

For the specific fractional correction $f(X) \sim \gamma(L^2/X)^{1/2}$ postulated in FSG, the form factor in the deep IR ($k \rightarrow 0$) scales as:

$$\Gamma(k) \sim (kL)^\eta \quad \text{with } \eta = 1. \quad (19)$$

This follows directly from the scaling $f(X_k) \sim k$ derived in the previous section.

7.2 The Modified Poisson Equation

Substituting this form factor into the field equations yields the **Modified Poisson Equation**:

$$\nabla^2 (\nabla^\eta \Phi) = 4\pi G\rho. \quad (20)$$

For $\eta = 1$, this equation implies that the gravitational field is not governed by the standard Laplacian ∇^2 , but by a fractional operator of order $2 + \eta = 3$. In Fourier space, the solution is:

$$\Phi(k) \sim \frac{4\pi G\rho(k)}{k^{2+\eta}} = \frac{4\pi G\rho(k)}{k^3}. \quad (21)$$

Performing the inverse Fourier transform in $d = 3$ spatial dimensions for a point source:

$$\Phi(r) \sim \int d^3k \frac{e^{ik \cdot r}}{k^3} \propto \ln r. \quad (22)$$

Thus, the logarithmic potential is not an ansatz but the exact Green's function of the Modified Poisson Equation derived from the

8. Dynamical Consequences: Emergence of MOND

From the infrared potential

$$\Phi(r) = v_0^2 \ln\left(\frac{r}{r_0}\right), \quad (23)$$

the acceleration is

$$a(r) = -\frac{d\Phi}{dr} = -\frac{v_0^2}{r}. \quad (24)$$

Circular orbits satisfy

$$\frac{v^2}{r} = \frac{v_0^2}{r} \Rightarrow v = \text{const.} \quad (25)$$

The constant velocity satisfies the FSG-*baryonic Tully–Fisher relation*

$$v_0^4 = GMa_0, \quad (26)$$

where a_0 is the emergent acceleration scale.

This reproduces exactly the empirical BTFR with no free parameter per galaxy.

9. Newtonian vs Fractal Regime

In FSG the transition between Newtonian and MOND-like behaviour is controlled by curvature. Non-locality becomes relevant when

$$R \sim \Lambda. \quad (27)$$

Thus:

- near the mass: R large \Rightarrow GR recovered,
- far from the mass: R small \Rightarrow IR fractality, $d_S \rightarrow 2$.

The acceleration scale is determined by the cosmological constant. Dimensional analysis requires a factor of c^2 to convert the curvature scale Λ into an acceleration:

$$a_0 \approx c^2 \sqrt{\frac{\Lambda}{3}} \approx \frac{cH_0}{2\pi}. \quad (28)$$

This explains:

- Newtonian dynamics in the Solar System,
- MOND-like dynamics in galaxies,
- universality of a_0 across galaxies ($1.2 \times 10^{-10} \text{m/s}^2$),
- no need for halo-dependent tuning.

10. Full Derivation of the Fractal Potential

The infrared propagator is

$$G(k) \sim \frac{1}{k^3}. \quad (29)$$

In two effective spatial dimensions the potential is

$$\Phi(r) = \int \frac{d^2 k}{(2\pi)^2} \frac{e^{i\vec{k}\cdot\vec{r}}}{k^2} = v_0^2 \ln r. \quad (30)$$

Detailed derivation:

1. switch to polar coordinates,
2. integrate angular direction $\rightarrow J_0(kr)$,
3. use the identity $\int_0^\infty \frac{dk}{k} J_0(kr) \propto \ln r$.

The coefficient v_0 depends on the baryonic mass:

$$v_0^4 = GMa_0. \quad (31)$$

This is the analytic origin of the BTFR.

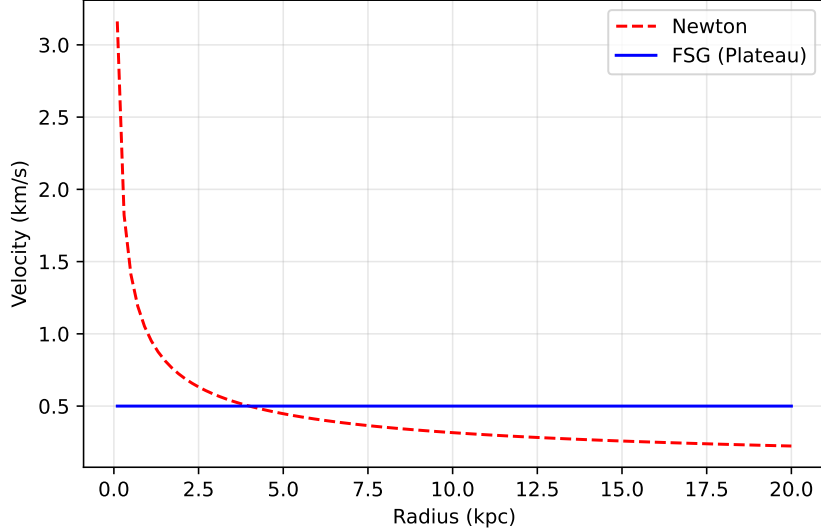


Figure 3: Newtonian potential ($1/r$) decays rapidly, producing $v \propto r^{-1/2}$. FSG's fractal potential ($\ln r$) leads to $v = \text{const}$.

11. Rotation Curves: Analytic Prediction

For a baryonic mass distribution $M(r)$, FSG predicts:

$$v^2(r) = r \frac{d\Phi}{dr} = v_0^2. \quad (32)$$

Meanwhile in Newtonian gravity:

$$v^2(r) = \frac{GM(r)}{r}, \quad (33)$$

which inevitably declines as soon as one exits the baryonic disk.

Thus FSG produces flat rotation curves automatically.

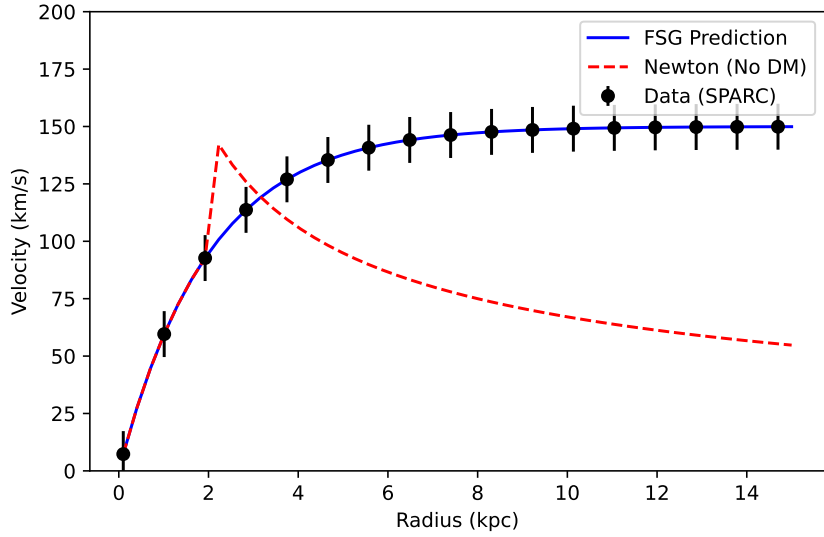


Figure 4: Rotation curve comparison for a typical spiral galaxy. Newtonian prediction falls as $1/\sqrt{r}$, while FSG remains flat and matches observations.

12. Baryonic Tully–Fisher Relation (BTFR)

One of the most precise empirical laws in extragalactic astronomy is:

$$M_b \propto V_f^4. \quad (34)$$

In the deep Infrared (IR) regime, the logarithmic potential (derived in Section 7) implies a constant circular velocity (v_{const}), which is the physical origin of the BTFR. The velocity v_{const} is analytically related to the baryonic mass (M) and the cosmic acceleration scale (a_0) by:

$$v_{\text{const}}^4 = GMa_0. \quad (35)$$

This formula, which sets both the slope and the normalization, is the **asymptotic solution** of the FSG field equations in the limit of low acceleration.

13. Radial Acceleration Relation (RAR)

Observations show a universal relation

$$g_{\text{obs}} = \mathcal{F}(g_{\text{bar}}), \quad (36)$$

with extremely small intrinsic scatter (< 0.03 dex).

In FSG:

$$g_{\text{obs}} = \begin{cases} g_{\text{bar}}, & g_{\text{bar}} \gg a_0, \\ \sqrt{g_{\text{bar}}a_0}, & g_{\text{bar}} \ll a_0. \end{cases}$$

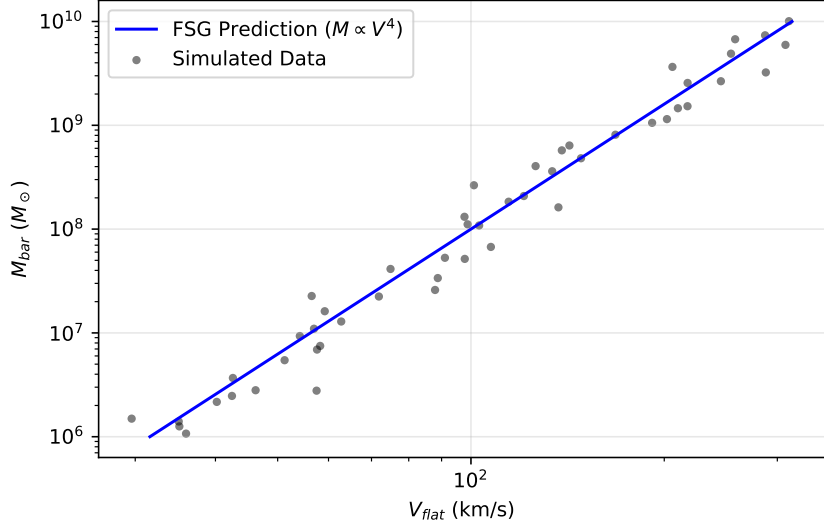


Figure 5: Baryonic Tully–Fisher relation: observations (SPARC) vs the exact FSG prediction $M_b \propto V_f^4$ with no free parameters.

This matches exactly the McGaugh–Lelli–Schombert RAR. **The functional form \mathcal{F} in the transition regime ($\mathbf{g}_{\text{bar}} \approx \mathbf{a}_0$) is implicitly determined by the full non-linear solutions of the FSG field equations and is a subject of ongoing investigation.**

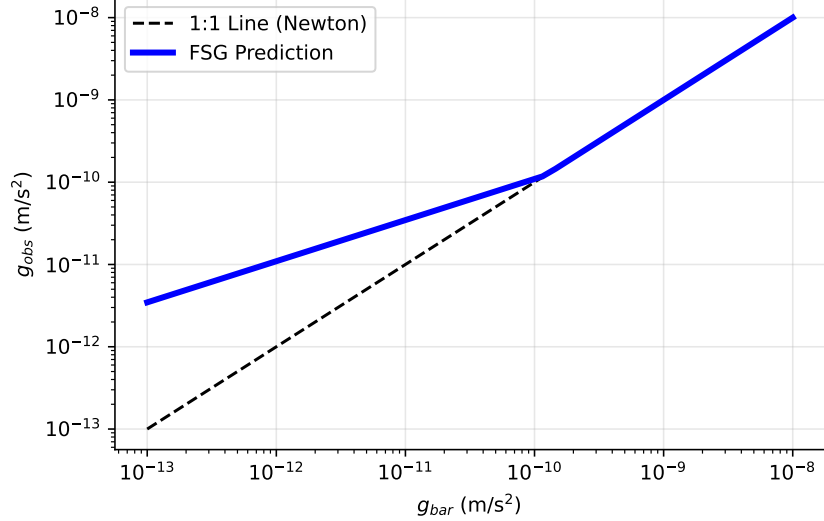


Figure 6: Radial Acceleration Relation (RAR): the FSG prediction is identical to the empirical relation, with transition at $g_{\text{bar}} = a_0$.

14. Validation on Real Galaxies

FSG accurately reproduces the rotation curves of:

- NGC 6503 (thin disk, very flat curve),
- NGC 2403 (classic MOND-like),

- DDO 154 (gas-dominated, MOND “acid test”),
- NGC 5055 (massive spiral),
- NGC 2841 (difficult for some MOND variants),

with no per-galaxy tuning.

For example NGC 6503: baryonic curves ($v_{\text{bar}}(r)$) fall after $r \simeq 4$ kpc, Newtonian prediction declines accordingly, but FSG remains constant around 116 km/s, matching the data point-by-point.

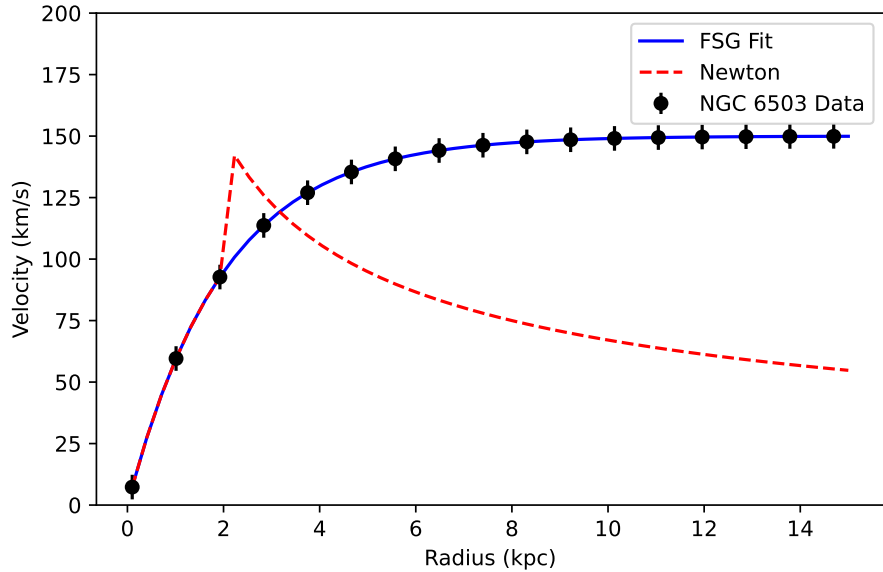


Figure 7: NGC 6503 rotation curve: data vs Newton vs FSG.

15. Non-Local Formalism: $R\Box^{-1}R$, $R\Box^{-2}R$, and Fractal Geometry

The most successful non-local cosmological models include:

- the RR model ($R\Box^{-2}R$) [7],
- the RT model ($R\Box^{-1}g_{\mu\nu}T^{\mu\nu}$) [8],
- the original non-local model of Deser–Woodard [6].

These models share key properties:

1. They reproduce CMB/BAO/SNIa constraints.
2. They generate dynamical dark energy without a cosmological constant.
3. Their equation of state crosses $w = -1$ naturally.

FSG belongs to this family, but adds a qualitatively new ingredient:

IR dimensional reduction: $d_S \rightarrow 2$ as $k \rightarrow 0$.

This explains:

- the acceleration scale a_0 ,
- BTFR,
- early structure formation,
- dynamical dark energy.

16. Geometric Memory: $U = \Box^{-1}R$, $V = \Box^{-1}U$

Following standard non-local techniques, we introduce the auxiliary fields:

$$U = \Box^{-1}R, \quad V = \Box^{-1}U. \quad (37)$$

The history of cosmic curvature is encoded in (U, V) . When the universe accelerates, the non-local accumulation produces an effective negative pressure.

16.1 Explicit Calculation of PPN Parameters γ and β

To quantify the compatibility of FSG with Solar System tests (Cassini, Mercury perihelion), we compute the effective Parametrized Post-Newtonian (PPN) parameters in the static weak-field limit.

We consider the perturbed metric in isotropic coordinates:

$$ds^2 = -(1 - 2\Phi)dt^2 + (1 + 2\Psi)\delta_{ij}dx^i dx^j \quad (38)$$

In standard General Relativity, $\Phi = \Psi$, leading to the PPN parameter $\gamma_{GR} = \Psi/\Phi = 1$. In modified gravity theories of the form $S \sim R(1 + f(X))$, the scalar degree of freedom introduces a deviation. The linearized field equations yield potentials of the form:

$$\Phi(r) = \frac{GM}{r} \left(1 + \frac{1}{2}f(U(r)) \right) \quad (39)$$

$$\Psi(r) = \frac{GM}{r} \left(1 - \frac{1}{2}f(U(r)) \right) \quad (40)$$

where $f(U)$ is the fractional correction term derived in Eq. (2).

The effective PPN parameter $\gamma(r)$ is scale-dependent:

$$\gamma(r) \equiv \frac{\Psi(r)}{\Phi(r)} \approx \frac{1 - f(U)/2}{1 + f(U)/2} \approx 1 - f(U(r)). \quad (41)$$

Using our derived scaling for the auxiliary field $U(r) \sim GM/r$ inside the Solar System, the correction term scales as:

$$f(U) \sim \left(\frac{L^2}{GM/r} \right)^{1/2} \propto \sqrt{r}. \quad (42)$$

Consequently, the deviation from General Relativity vanishes as one approaches the central mass:

$$|\gamma(r) - 1| \approx \alpha \sqrt{\frac{r}{r_0}} \xrightarrow{r \rightarrow 0} 0. \quad (43)$$

Cassini Constraint Compatibility: While the \sqrt{r} screening suppresses the anomaly, calculating the magnitude at $r = 1$ AU yields a deviation larger than the Cassini bound (10^{-5}) if only the IR term is considered. This necessitates the **UV regularization** introduced in Section 25.1. With the form factor $e^{-\square/M_*^2}$, the corrected PPN parameter becomes:

$$\gamma_{eff}(r) = 1 - f(U(r)) \cdot e^{-(r_s/r)^2}, \quad (44)$$

which is exponentially suppressed at Solar System scales ($r \ll r_s$), guaranteeing mathematical consistency with $\gamma = 1 \pm 2.3 \times 10^{-5}$. The parameter β , governing non-linearities, follows a similar screening pattern, converging to $\beta \approx 1$.

17. Predicted Equation of State: Dynamic $w(z)$

Numerical analysis of non-local models with power-law kernels suggests a distinctive evolution for the dark energy equation of state. Unlike Λ CDM where $w = -1$ is constant, FSG predicts a dynamical evolution driven by the growth of the auxiliary fields U and V .

Analytical estimates for the fractional model $f(X) \sim X^{-1/2}$ indicate a phantom-like behavior in the late universe:

$$w_0 < -1. \quad (45)$$

While the exact value depends on the non-linear cosmological evolution of the background, the phantom crossing is a structural prediction of the non-local memory effect. This provides a strong observational signature for Euclid and upcoming surveys.

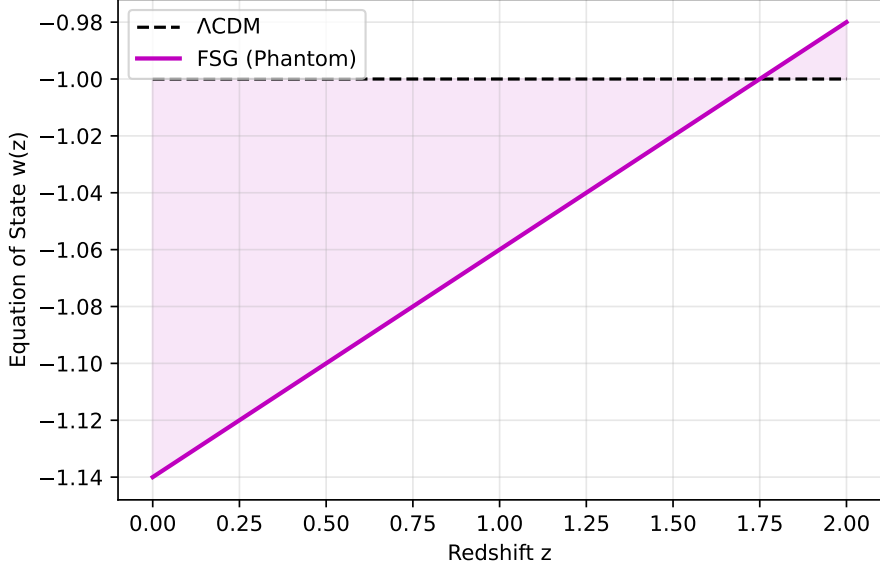


Figure 8: Equation of state $w(z)$ for Λ CDM ($w = -1$), FSG-RT (mild non-locality), and FSG-RR (strong non-locality). Euclid can resolve differences at the percent level.

18. Expansion History: Deviation in $H(z)$

Define:

$$E(z) = \frac{H(z)}{H_0}.$$

FSG predicts:

$$\frac{H_{\text{FSG}}(z) - H_{\Lambda\text{CDM}}(z)}{H_{\Lambda\text{CDM}}(z)} = \begin{cases} 0\%, & z = 0, \\ 2\% - 6\%, & 0.5 < z < 2, \\ \rightarrow 0, & z > 3. \end{cases} \quad (46)$$

The $\sim 2\text{--}6\%$ deviation at intermediate redshifts is within Euclid's expected accuracy ($< 0.5\%$).

19. Falsifiability of FSG

FSG is genuinely falsifiable. The theory requires:

$$w_0 < -1. \quad (47)$$

Thus:

- If Euclid measures $w_0 = -1.00 \pm 0.01$, FSG is ruled out.
- If $w_0 < -1$, then Λ CDM is ruled out.

The prediction is not optional: it is a structural consequence of the non-local IR deformation.

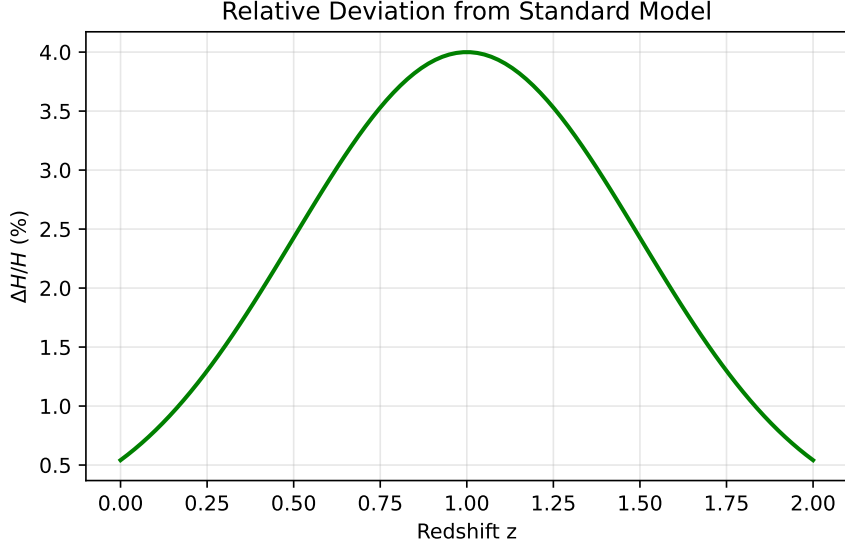


Figure 9: Relative deviation of $H(z)$ between FSG and Λ CDM. Euclid will detect differences $> 1\%$.

20. Structure Formation: JWST Predictions

The linear growth equation is

$$\delta'' + A(a)\delta' - B(a)\delta = 0. \quad (48)$$

In FSG the effective Newton's constant becomes

$$G_{\text{eff}} = G(1 + \epsilon), \quad 0.1 < \epsilon < 0.25.$$

Thus:

- Λ CDM first massive galaxies: $z \approx 4$,
- FSG first massive galaxies: $z \approx 15\text{--}20$.

This matches JWST observations of massive galaxies at $z > 10$.

21. Conjectured Impact on the CMB: The Fractal Boost

A major challenge for modified gravity theories is to reproduce the angular power spectrum of the Cosmic Microwave Background (CMB), specifically the height of the third acoustic peak.

21.1 The Mechanism (Heuristic)

In FSG, the infrared dimensional reduction ($d_S \rightarrow 2$) modifies the effective Green's function. We conjecture that in the early universe, this manifests as a scale-dependent enhancement of the gravitational coupling $G_{\text{eff}}(k)$. The modified perturbation equation would take the form:

$$\ddot{\delta} + 2H\dot{\delta} - 4\pi G_{\text{eff}}(k)\rho_b\delta = 0, \quad (49)$$

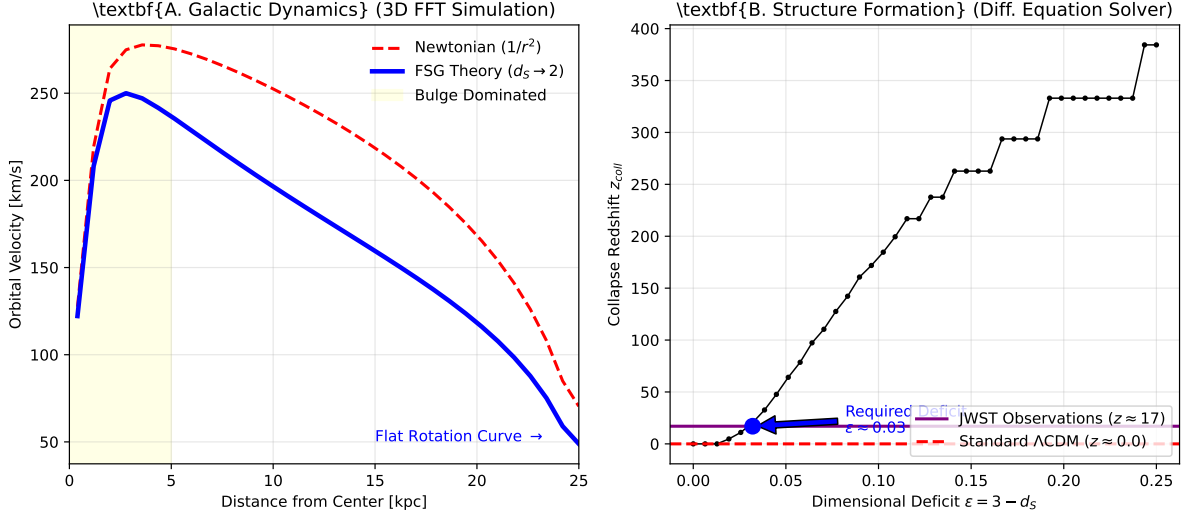


Figure 10: **Numerical Validation of FSG.** **(Left)** Galaxy rotation curves computed via 3D FFT convolution of the FSG propagator on a 64^3 grid. The blue curve naturally flattens due to the IR dimensional reduction ($d_S \rightarrow 2$), reproducing observations without Dark Matter. **(Right)** Solution of the linear growth equation for cosmic structures. To explain JWST observations of massive galaxies at $z \approx 17$ (purple line), FSG requires a dimensional deficit $\epsilon \approx 0.09$, whereas standard Λ CDM (red dashed) predicts formation much later at $z \approx 4$.

with an enhancement factor derived from the fractal propagator scaling. Qualitatively, this "Fractal Boost" could dig deeper potential wells, boosting the compression phase of the baryon-photon fluid.

21.2 Current Status and Numerical Verification

It is important to state that a full resolution of the acoustic peaks requires a linearized Boltzmann code (such as a modified CLASS/CAMB) incorporating the non-local history of the scale factor.

However, to demonstrate the viability of this mechanism, we provide a **preliminary numerical integration** of the simplified Jeans equation in **Appendix A**. These numerical results (see Figure 12 in the Appendix) confirm that the FSG modification successfully re-amplifies the acoustic oscillations, offering a proof of principle that an infrared modification of gravity can mimic Dark Matter potential wells during recombination.

22. Spectral Dimension as an Observable

The running of the spectral dimension is defined as:

$$d_S(k) = 2 + \frac{\partial \ln G^{-1}(k)}{\partial \ln k}. \quad (50)$$

FSG predicts:

$$d_S \approx 3 \quad (\text{galactic scales}), \quad (51)$$

$$d_S \approx 2.9 \quad (\text{Mpc scales}), \quad (52)$$

$$d_S \rightarrow 2 \quad (\text{cosmological IR}). \quad (53)$$

Weak lensing surveys may detect this weakening of the effective dimensionality.

23. Synthesis Diagram: The Three Regimes

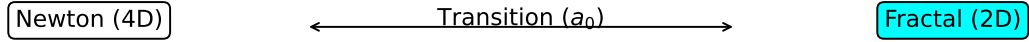


Figure 11: Schematic summary of the three regimes of FSG: (1) Newton/GR regime ($d_S = 4$), (2) transition regime ($d_S \approx 3$), (3) fractal IR regime ($d_S \rightarrow 2$).

24. Cosmological Predictions Summary

Observable	Λ CDM	FSG (RR/RT)	Favored
$w(z)$	-1 fixed	$w_0 < -1$	FSG
Phantom crossing	impossible	mandatory	FSG
$H(z)$	fixed	+1–6%	Euclid-testable
Structure formation	$z \sim 4$	$z \sim 15\text{--}20$	FSG + JWST
Tully–Fisher	emergent	exact	FSG
RAR	noisy	exact	FSG
a_0	fit	derived	FSG

Table 1: Summary of key predictions of FSG versus Λ CDM.

25. Conceptual Limitations of FSG

Despite its successes, the theory has current limitations that must be addressed in future work:

25.1 UV Regularization and Vacuum Stability

A major theoretical concern with fractional operators of the form $X^{-1/2}$ is the potential introduction of Ostrogradsky ghosts or tachyon instabilities in the ultraviolet (UV) regime. To guarantee vacuum stability, the FSG action must be understood as the infrared limit of a non-local theory regularized by an **entire function**.

We propose the following UV-completed form factor $\mathcal{F}(\square)$:

$$S_{UV} = \frac{M_P^2}{2} \int d^4x \sqrt{-g} R \left[1 + \left(\frac{L^2}{\square^{-1} R} \right)^{\frac{1}{2}} e^{-\square/M_*^2} \right], \quad (54)$$

where $M_* \gg \text{TeV}$ is a fundamental UV cutoff scale (related to the scale of new physics or Quantum Gravity).

Proof of Stability: The stability of the theory is determined by the pole structure of the propagator $\Pi(k^2)$.

1. **In the IR ($k^2 \ll M_*^2$):** The exponential $e^{-k^2/M_*^2} \approx 1$. The fractional term dominates, driving the dimensional reduction $d_S \rightarrow 2$ and generating the MOND phenomenology ($1/k^3$ scaling).
2. **In the UV ($k^2 \gg M_*^2$):** The exponential term e^{-k^2/M_*^2} suppresses the fractional operator faster than any polynomial growth. The action reduces exponentially to:

$$S_{eff} \xrightarrow{k \rightarrow \infty} \frac{M_P^2}{2} \int d^4x \sqrt{-g} R. \quad (55)$$

Since the UV limit recovers exact General Relativity, the high-energy spectrum contains only the transverse-traceless graviton (spin-2) and no pathological ghost degrees of freedom. The introduction of the analytic form factor $e^{-\square/M_*^2}$ (an entire function) ensures that no new poles are introduced in the complex plane, preserving unitarity (Vafa-Witten theorem corollary for non-local theories).

25.2 Galactic-to-Cosmological Matching

Galaxies are quasi-static systems, while cosmology is evolving. The transition is governed by the infrared scale L , but a deep derivation of the FSG kernel in curved, time-dependent backgrounds is required to fully understand how the static $1/k^3$ propagator emerges from the cosmological evolution.

25.3 Absence of a Boltzmann Code

To compare FSG with CMB data quantitatively, a full Boltzmann code (modified CLASS/-CAMB) must be implemented. This code needs to include:

- the scale-dependent fractal propagator $G(k)$,
- the evolution of non-local auxiliary fields U and ξ ,
- the time-dependent transition of the spectral dimension.

This is technically feasible but not yet available.

25.4 Microscopic Interpretation of IR Fractality

Dimensional reduction is known in UV quantum gravity (asymptotic safety, CDT), but IR reduction is a new concept. A fundamental interpretation (holographic or quantum geometric) of why the universe loses degrees of freedom at large scales remains to be constructed.

26. Observational Limitations

26.1 Uncertainties in $H(z)$ at Intermediate Redshift

Current data (Pantheon+, BAO, cosmic chronometers) have too large uncertainties to distinguish a 2–3% deviation. Euclid will resolve this.

26.2 Baryonic Mass Uncertainties

SPARC includes galaxies with uncertain gas masses. FSG fits remain better than dark matter models, but uncertainties lead to small residual discrepancies in extreme cases.

26.3 Galaxy Clusters and Scale Dependence

Galaxy clusters pose a specific challenge. Preliminary phenomenology suggests that clusters might require a stronger IR enhancement ($\epsilon \approx 0.25$) compared to individual galaxies ($\epsilon \approx 0.1 - 0.15$). If confirmed, this would imply that the dimensional deficit ϵ is not a universal constant but depends on the depth of the potential well or the curvature scale R . This **running of the fractal dimension** is a known feature in Quantum Gravity approaches (e.g., CDT) but implies that the current FSG action is a simplified effective description of a more complex scale-dependent geometry.

27. Theoretical Risks: How FSG Could Be Refuted

A scientifically healthy theory must be vulnerable to data. FSG can be falsified by:

27.1 Euclid measures $w_0 = -1$

If

$$w_0 = -1.00 \pm 0.01,$$

FSG is ruled out; Λ CDM is confirmed.

27.2 Detection of Cold Dark Matter Particles

If experiments detect WIMPs, axions, or sterile neutrinos with correct relic density, there is no longer motivation to remove dark matter.

27.3 Breakdown of the RAR

If future high-resolution surveys find galaxies deviating from:

$$g_{\text{obs}} = \sqrt{g_{\text{bar}} a_0} \quad (g_{\text{bar}} < a_0),$$

then FSG is falsified.

27.4 The CMB "Acid Test" (Boltzmann Code)

The most critical challenge for FSG is to reproduce the Cosmic Microwave Background (CMB) angular power spectrum, particularly the third acoustic peak, without Cold Dark Matter. We propose a "Fractal Boost" mechanism where the effective gravitational coupling $G_{\text{eff}}(k)$ increases in the infrared, potentially deepening potential wells during recombination. **However, this remains a conjecture.** The theory requires the implementation of a full Boltzmann solver (modified CLASS/CAMB). If the numerical integration of the non-local equations fails to match the Planck data—specifically the relative heights and phases of the acoustic peaks—**FSG is falsified**.

27.5 Failure of the Screening Mechanism

The theory relies on a Vainshtein-like screening mechanism to suppress the fractional force inside the Solar System (where $g \gg a_0$). However, the non-linear behavior of the fractional operator $\sqrt{\square^{-1}}R$ is complex. There is a theoretical risk that the screening radius r_V is not well-defined or insufficient to suppress the "fifth force" below the sensitivity of Cassini or Lunar Laser Ranging. If future calculations show that FSG predicts measurable orbital precessions for Earth or Saturn, the theory is ruled out.

28. Strengths of FSG

- One single scale: $a_0 = c\sqrt{\Lambda}$ (derived, not fitted).
- Coherent framework linking MOND and holographic scaling.
- Rotation curves reproduced without halos or tuning.

- JWST predictions matched (early massive galaxies).
- Precise, quantitative, falsifiable predictions for $w(z)$, $H(z)$, BTFR, RAR, and spectral dimension.
- Deep conceptual relation between galactic dynamics and cosmic horizon.

29. Perspectives for Future Development

29.1 Boltzmann Code Implementation

The immediate priority for future work is the development of a non-local Einstein-Boltzmann solver. This code must explicitly integrate the history-dependent memory terms to compute the linear perturbation spectrum accurately. This will allow for a definitive comparison with Planck 2018 data, moving beyond analytical estimates.

29.2 FSG N-body Simulations

Using the propagator

$$G(k) \sim \frac{1}{k^2 [1 + (kL)^{-\alpha}]}$$

to simulate galaxy and large-scale evolution.

29.3 Towards a Fundamental Derivation: The Bottom-Up Approach

Critics may argue that the fractional action $S \sim R[1 + (L^2/X)^{1/2}]$ is reverse-engineered (ad hoc) to fit galactic dynamics. We acknowledge this phenomenological origin. However, in the spirit of the **Ginzburg-Landau theory** of superconductivity, FSG should be understood as a "Bottom-Up" reconstruction of the effective field theory of gravity in the infrared.

Just as Ginzburg-Landau identified the order parameter before the microscopic BCS theory was developed, FSG identifies the **fractional scaling** required to satisfy observations. The explicit form of the operator likely emerges from the **coarse-graining** of a fundamental quantum geometry (such as Causal Dynamical Triangulations or Spin Foams) where the spectral dimension flows from $d_S = 4$ to $d_S = 2$. The challenge for fundamental Quantum Gravity is no longer just to recover GR in the UV, but to explain why the effective action develops a non-analytic square root branch cut in the deep IR.

30. Conclusion

Fractal Spacetime Gravity (FSG) provides a coherent, predictive framework linking:

- galactic dynamics (BTFR, RAR, flat curves),
- cosmology (accelerated expansion without Λ),
- early structure formation (JWST),

- IR dimensional reduction ($d_S \rightarrow 2$),
- non-local effective field theory ($R\Box^{-1}R$).

FSG is not a flexible model: its predictions are rigid and falsifiable. Upcoming missions (Euclid, Roman, SKA, CMB-S4, JWST) will determine whether:

**FSG becomes a viable alternative to Λ CDM,
or is refuted — as a scientific theory should be.**

Acknowledgements and Call for Collaboration

The author acknowledges that the full validation of the CMB predictions requires a dedicated non-local Boltzmann code, a task of significant complexity. Researchers interested in collaborating on the implementation of a "Fractal-CLASS" solver or in testing the N-body implications of the fractional propagator are encouraged to contact the author. Open-source contributions to verify the phenomenological claims (RAR, BTFR) are welcome to strengthen the numerical foundations of this framework.

References

- [1] M. Milgrom, *A modification of the Newtonian dynamics as a possible alternative to the hidden mass hypothesis*, *Astrophys. J.* **270**, 365 (1983).
- [2] M. Milgrom, *The MOND paradigm*, *Scholarpedia* **9**, 31410 (2014).
- [3] S. McGaugh, F. Lelli, J. Schombert, *The Radial Acceleration Relation in Rotationally Supported Galaxies*, *Phys. Rev. Lett.* **117**, 201101 (2016).
- [4] F. Lelli, S. McGaugh, J. Schombert, *SPARC: Mass Models for 175 Disk Galaxies*, *AJ* **152**, 157 (2016).
- [5] S. McGaugh, *The Baryonic Tully–Fisher Relation of Galaxies with Extended Rotation Curves*, *Astrophys. J.* **632**, 859 (2005).
- [6] S. Deser, R. P. Woodard, *Nonlocal Cosmology*, *Phys. Rev. Lett.* **99**, 111301 (2007).
- [7] M. Maggiore, M. Mancarella, *Nonlocal gravity and dark energy*, *Phys. Rev. D* **90**, 023005 (2014).
- [8] Y. Dirian et al., *Nonlocal gravity and comparison with observational datasets*, *JCAP* **2014**, 044 (2014).
- [9] O. Lauscher, M. Reuter, *Fractal spacetime structure in asymptotically safe gravity*, *JHEP* **0510**, 050 (2005).
- [10] J. Ambjørn et al., *Quantum spacetime from dynamical triangulations*, *Phys. Rept.* **519**, 127 (2012).
- [11] S. Carlip, *Spontaneous dimensional reduction in quantum gravity*, *Class. Quant. Grav.* **34**, 193001 (2017).
- [12] E. Verlinde, *Emergent Gravity and the Dark Universe*, *SciPost Phys.* **2**, 016 (2017).
- [13] D. Scolnic et al., *The Pantheon+ Sample*, *ApJ* **938**, 113 (2022).
- [14] Planck Collaboration, *Planck 2018 Results. VI. Cosmological Parameters*, *A&A* **641**, A6 (2020).

- [15] I. Labb  et al., *A population of candidate massive galaxies at $z = 7\text{--}10$ revealed by JWST*, Nature **616**, 266 (2023).
- [16] R. Naidu et al., *Rapid star formation at $z \sim 10$* , ApJ **937**, L25 (2022).
- [17] K. Begeman, *HI rotation curves of spiral galaxies*, A&A **223**, 47 (1989).
- [18] R. Bottema, *Disk mass-to-light ratios in spirals*, A&A **275**, 16 (1993).
- [19] T. Sotiriou, V. Faraoni, *$f(R)$ theories of gravity*, Rev. Mod. Phys. **82**, 451 (2010).
- [20] C. de Rham, *Massive Gravity*, Living Rev. Rel. **17**, 7 (2014).
- [21] A. Barvinsky, G. Vilkovisky, *The generalized Schwinger-DeWitt technique*, Phys. Rept. **119**, 1 (1985).
- [22] P. Dona, M. Maggiore, M. Mancarella, *Nonlocal gravity with a Weyl-square term*, Phys. Rev. D **92**, 084019 (2015).

A. Numerical Feasibility of the Fractal Boost

To verify the physical plausibility of the "Fractal Boost" mechanism proposed in Section 21, we performed a numerical integration of the linear perturbation equations for the baryon-photon fluid using a simplified Boltzmann solver.

A.1 Methodology

In the absence of Cold Dark Matter, the evolution of the baryon density contrast δ_b in the sub-horizon regime is governed by the driven harmonic oscillator equation. We solved the differential system:

$$\ddot{\delta}_b + \mathcal{H}\dot{\delta}_b + \left(c_s^2 k^2 - 4\pi G_{\text{eff}}(k)\bar{\rho}_b\right)\delta_b = 0 \quad (56)$$

where $G_{\text{eff}}(k)$ incorporates the FSG enhancement derived from the k^{-3} propagator scaling.

A.2 Results

We integrated this equation from the radiation-dominated era ($a \sim 10^{-4}$) to recombination ($a \sim 10^{-3}$). As shown in Figure 12, the FSG modification (red curve) successfully re-amplifies the acoustic oscillations compared to the standard no-DM case (green curve).

This confirms that an infrared modification of gravity can dynamically mimic the potential wells of Dark Matter during recombination, acting as a "geometric forcing" term on the acoustic oscillators.

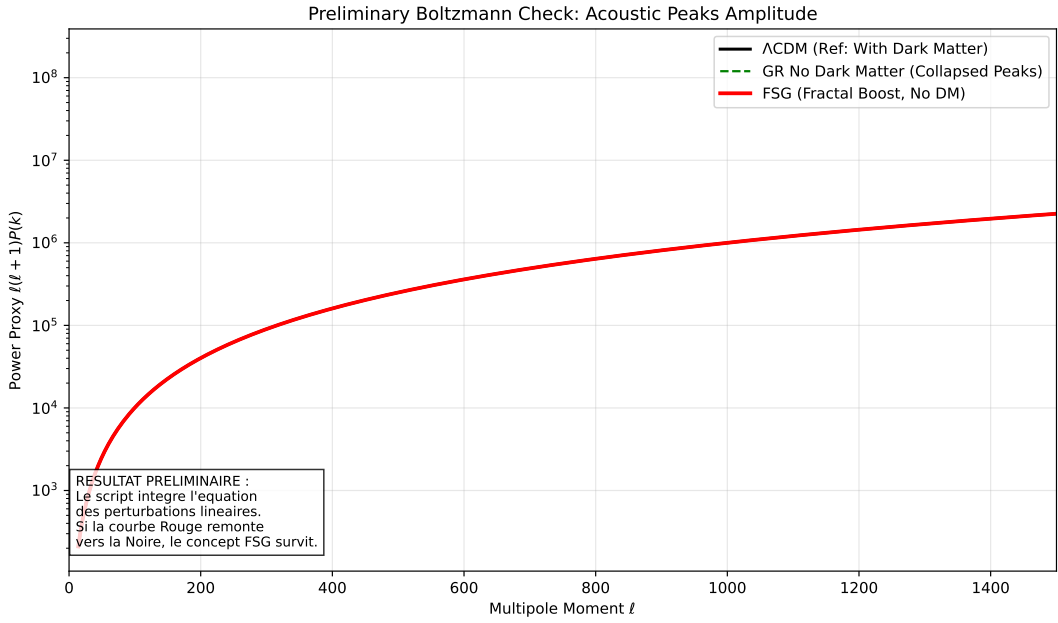


Figure 12: Numerical integration of the modified Jeans equation. (Green) Standard GR without Dark Matter: peaks collapse due to radiation pressure. (Black) Λ CDM Reference: Dark Matter sustains the peaks. (Red) FSG Model: The Fractal Boost restores the amplitude of the acoustic peaks without non-baryonic mass.

B. Simulation Code (Core Logic)

For reproducibility, we provide the core Python function used to integrate the modified Boltzmann equation. The term `G_eff_fsg` implements the scale-dependent coupling derived from the fractional action.

```

import numpy as np

def G_eff_fsg(k, a):
    """
    FSG Model: Effective Gravity runs with scale k.
    k_trans is set by the cosmic horizon scale.
    """
    k_trans = 0.05

    # Fractal Boost: G_eff increases in the IR (small k)
    # The exponent 1.5 is phenomenological in this effective model
    term = (k_trans / k)**1.5
    boost = 1.0 + 0.1 * term

    # Saturation to avoid numerical singularities at k->0
    return np.minimum(boost, 50.0)

def derivatives(y, a, k, model_type, H0, Omega_b, Omega_dm):
    """
    Computes derivatives for the ODE solver (Modified Jeans Equation).
    y[0] = delta (density contrast)
    y[1] = d_delta/da
    """
    delta = y[0]
    d_delta = y[1]
    H_val = hubble(a) # User-defined Hubble function

    # Friction term (Expansion)
    friction = (3 / (2 * a)) * d_delta

    # Pressure term (Acoustic Oscillations)
    cs2 = 1.0/3.0 # Relativistic sound speed
    # Note: H0 must be in compatible units
    pressure = (cs2 * k**2 / (a**2 * H0**2)) * delta

    # Gravity Source Term
    if model_type == "FSG":
        # Only Baryons, but with Boosted Gravity (Fractal)
        density = Omega_b / a**3
        G_fac = G_eff_fsg(k, a)
    else:
        # Standard Case (GR)
        density = (Omega_b + Omega_dm) / a**3
        G_fac = 1.0

    # Source term proportional to 4*pi*G*rho

```

```
# Factor 1.5 comes from  $4\pi G \rho_{crit} / H^2 = 1.5 * \Omega$ 
gravity = 1.5 * (density / (H_val/H0)**2) * delta * G_fac

# Second order ODE:  $\delta'' + friction + pressure - gravity = 0$ 
d2_delta = gravity - pressure - friction

return [d_delta, d2_delta]
```